JBC Papers in Press. Published on July 24, 2006 as Manuscript M605850200
The latest version is at http://www.jbc.org/cgi/doi/10.1074/jbc.M605850200

DENMOTOXIN: A THREE-FINGER TOXIN FROM COLUBRID SNAKE *BOIGA DENDROPHILA* (MANGROVE CATSNAKE) WITH BIRD-SPECIFIC ACTIVITY

Joanna Pawlak‡, Stephen P. Mackessy§, Bryan G. Fry‡¶, Madhav Bhatia‖, Gilles Mourier†, Carole Fruchart-Gaillard†, Denis Servent†, Renée Ménez†, Enrico Stura†, André Ménez† and R. Manjunatha Kini‡#*

From the: ‡Department of Biological Sciences, Faculty of Science, National University of Singapore, Singapore 117543; §School of Biological Sciences, University of Northern Colorado, 501 20th St., CB 92, Greeley, CO 80639-0017, USA, ¶Current address: Australian Venom Research Unit, School of Medicine, University of Melbourne, Parkville, Victoria 3010, Australia; ‖Department of Pharmacology, Faculty of Medicine, National University of Singapore, Singapore 117543; †Département d'Ingénierie et d'Etudes des Protéines, Commissariat à l'Energie Atomique, Gif-sur-Yvette Cedex 91191, France; #Department of Biochemistry and Molecular Biophysics, Medical College of Virginia, Virginia Commonwealth University, Richmond VA 23298, USA

Running title: pharmacological and structural characterization of denmotoxin

*Address for correspondence: R. Manjunatha Kini, Protein Science Laboratory, Department of Biological Sciences, Faculty of Science, National University of Singapore, Science Drive 4, Singapore 117543, Tel. 65-6516-5235; Fax. 65-6779-2486; E-Mail: dbskinim@nus.edu.sg

***Boiga dendrophila* (Mangrove Catsnake) is a colubrid snake, which lives in Southeast Asian lowland rainforests and mangrove swamps, and which preys primarily on birds. We have isolated, purified and sequenced a novel toxin from its venom, which we named denmotoxin. It is a monomeric polypeptide of 77 amino acid residues and five disulphide bridges. In organ bath experiments it displayed potent postsynaptic neuromuscular activity and irreversibly inhibits the indirectly stimulated twitches in chick biventer cervicis nerve-muscle preparations. In contrast, it induced much smaller and readily-reversible inhibition of the electrically evoked twitches in mouse hemidiaphragm nerve-muscle preparations. More precisely, the chick $\alpha_1\beta\gamma\delta$ muscle nicotinic acetylcholine receptor is 100-fold more susceptible as compared to mice. These data indicate that denmotoxin has a bird-specific postsynaptic activity. We chemically synthesized denmotoxin, crystallized it, and solved its crystal structure at 1.9 Å by molecular replacement method. The toxin structure adopts a non-conventional three-finger fold with an additional (fifth) disulphide bond in the first loop, and seven additional residues at its NH_2-terminus, which is blocked by a pyroglutamic acid residue. This is the first crystal structure of a three-finger toxin from colubrid snake venom and the first fully characterized bird-specific toxin. Denmotoxin illustrates the relationship between toxin specificity and the primary prey type that constitutes the snake's diet.**

Three-finger toxins (3FTXs) form one of the most abundant, well recognized families of snake venom proteins. They share similar structure and are characterized by three β-stranded finger-like loops, emerging from a globular core and stabilized by four conserved disulfide bridges. An additional disulfide linkage may sometimes be present in the first (non-conventional toxins) or the second loop (long-chain α-neurotoxins and κ-toxins) (1-5). All 3FTXs are monomers except for κ-toxins, which are non-covalent, homodimers isolated from *Bungarus* venoms. Minor structural differences in the three-finger fold, namely the number of β-strands, overall morphology of the loops, differential lengths of turns or of the C-terminal tails (6) leads to the recognition of varied targets and modulates the toxicity and specificity (7). Hence, 3FTXs affect a broad range of molecular targets such as α1 (short- and long-chain α-neurotoxins), α7 (long-chain α-neurotoxins), or α3 and α4 (κ-toxins) nicotinic

acetylcholine receptors (nAChRs) (4;5), muscarinic acetylcholine receptors (muscarinic toxins) (8), L-type calcium channel (calciseptine and FS2 toxin) (9;10), integrin $\alpha_{IIb}\beta_3$ (dendroaspin) (11;12), integrin $\alpha_v\beta_3$ (cardiotoxin A5) (13), acetylcholinesterase (fasciculins) (14), phospholipids and glycospingolipids (cardiotoxins) (15), and blood coagulation protein factor VIIa (16). As the interaction with such a broad spectrum of target proteins results in a variety of pharmacological effects, the understanding of the physiological role and mechanism of action supported by the architecture of 3FTXs could be of a great value in the development of novel research tools or rational drug design. For instance, studies with α-bungarotoxin led to a detailed characterization of the muscle nAChR helping to elucidate the fundamental underlying mechanisms involved in neuromuscular transmissions (17).

3FTXs were thought to occur only in the venoms of the snake family Elapidae. But recently, our lab reported the first colubrid snake venom toxin (α-colubritoxin from *Coelognathus radiatus*), a reversible antagonist of chick muscle nAChRs (18). The large polyphyletic family Colubridae consists of approximately two-thirds of the described species of the advanced snakes and includes more than 700 different venomous species (19;20). Colubrid snakes possess a venom gland (the Duvernoy's gland) with a common duct extending to the posterior lingual region of the maxilla, commonly associated with a grooved or enlarged posterior maxillary teeth. Relatively little is known of the chemistry, toxicology and immunology of colubrid venoms and a more thorough investigation of colubrid venom components holds great promise for discovering new bio-active compounds (21;22).

In this paper, we report the isolation, purification, and pharmacological and structural characterization of a novel bird-specific neurotoxin, denmotoxin, one of the major venom components of Mangrove Catsnake (*Boiga dendrophila*). Denmotoxin produced a virtually irreversible block of chick muscle $\alpha_1\beta\gamma\delta$ nAChRs, whereas it produced a much weaker, readily reversible block of mouse muscle $\alpha_1\beta\gamma\delta$ nAChRs. In addition to pharmacological and biochemical studies, we have established a chemical synthesis and refolding protocol for synthetic denmotoxin and solved the high resolution crystal structure of the protein. Denmotoxin has great potential to become a model for a better understanding of the mechanisms of species-specificity as well as reversible binding of venom neurotoxins.

EXPERIMENTAL PROCEDURES

Materials - Most chemicals and drugs (including carbamylcholine chloride, d-turbocurarine chloride, and neostigmine bromide) were purchased from Sigma (St. Louis, MO, USA). Trypsin and Lys-C endopeptidase were purchased from Wako Pure Chemicals (Osaka, Japan) and *Pfu* pyroglutamate aminopeptidase from Takara Biochemicals (Tokyo, Japan). Acetonitrile (ACN) was obtained from Merck KGaA (Darmstadt, Germany) and reagents for protein sequencing were from Applied Biosystem (Foster City, CA, USA). Chromatography columns: μRPC C2/C18 (10 μ, 120 Å, 2.1 x 100 mm) and Superdex 30 Hiload gel filtration column (1.6 x 60 cm) - Amersham Pharmacia (Uppsala, Sweden); RP-Jupiter C18 (5 μ, 300 Å, 1 x 150 mm) - Phenomenex (Torrance, CA, USA); UNO S-6 cation exchange column - Bio-Rad Laboratories (Hercules, CA, USA); and Discovery®BIO Wide Pore C5 (5 μ, 300 Å, 10 x 250 mm) and Discovery®BIO Wide Pore C5 (5 μ, 300 Å, 4.6 x 150 mm) - Sigma (St. Louis, MO, USA). RNA isolation (RNeasy® mini kit), one-step RT-PCR, Qiaquick® PCR purification, gel extraction, plasmid isolation miniprep kits, PCR cloning kit and Hot Start *Taq* Polymerase kit were purchased from Qiagen (Valencia, CA, USA). The ABI PRISM BigDye terminator cycle sequencing ready reaction kit was purchased from Applied Biosystems (Foster City, CA, USA). Gene-specific primers were custom synthesized by 1st BASE (Singapore). DNA ladder 1 Kb Plus was purchased from GIBCO BRL (Carlsbad, CA, USA). *Eco*RI restriction endonuclease was obtained from New England Biolabs (Beverly, MA, USA). Luria Bertani broth and agar were purchased from Q.BIOgene (Irvine, CA, USA). Water was purified with a MilliQ system (Millipore, Billerica, MA, USA). For protein synthesis, protected amino acid derivatives, resins, dicyclohexylcarbodiimide and N-hydroxybenzotriazole (HOAT) were from Nova-Biochem (Meudon, France). Piperidine, N-methylpyrrolidone, dichloromethane, methanol,

trifluroacetic acid (TFA) and tert-butyl methyloxide were from SDS (Peypin, France). Tris (2-carboxyethyl)-phosphine hydrochloride (TCEP) was from Pierce (Rockford, Illinois, USA).

Snakes venoms - *B. dendrophila* venom was extracted as described previously (23) from snakes originating from Sulawesi, Indonesia. *Bungarus multicinctus* venom was obtained from Venom Supplies Pte Ltd (Tanunda, SA, Australia) and α-bungarotoxin was purified using standard method (24).

Animals - Swiss-Webster albino mice (32 ± 2 g body weight) were purchased from the Laboratory Animals Center, National University of Singapore (Sembawang, Singapore) and kept in the Pharmacology Department Animal Holding Unit (AHU #01-03). Paper pellet bedding as well as food was purchased from Geln Forrest Stockfeeders, WA, Australia. Food and water were available *ad lib.* The animals were housed 5 per cage in a light-controlled room (12 h light/dark cycles), at 23 °C and 60% relative humidity.
Six to ten day old domestic chickens (*Gallus domesticus*) were purchased from an agricultural farm in Singapore and delivered on the day of experiment. Experimental animals were euthanized by exposure to 100% CO_2 in accordance with the most recent recommendations of the American Veterinary Medical Association (AVMA) Panel on Euthanasia, utilizing procedures that produce rapid unconsciousness and subsequent humane death. Animals were handled according to the Animals and Birds (Care and Use of Animals for Scientific Purposes) Rules 2004, the National Advisory Committee for Laboratory Animal Research (NACLAR) Guidelines (IACUC protocol # 776a/05) and the University of Northern Colorado IACUC (protocol #9204.1).

Protein purification - Previously, we had performed LC/MS crude venom profiling of *B. dendrophila* venom (25) to identify venom complexity and to predict composition of venom proteins. A major protein component was purified from the venom using a two-step process including cation exchange and reversed-phase HPLC. Crude venom was applied to a cation exchange column UNO S-6 attached to ÄKTA Purifier system (Amersham Pharmacia, Uppsala, Sweden) and separated into fractions with a linear gradient of 0 to 50% of solvent B over 50 min (A = 50 mM Tris-HCl, pH 7.5; B = 1 M NaCl in 50 mM Tris-HCl, pH 7.5). The pooled fractions containing the protein of interest were applied to an RP-HPLC Jupiter C18 (5 µ, 300 Å, 1 x 150 mm) column using the same chromatographic system and eluted with a linear gradient of 30 to 40% solvent B over 80 min (A = 0.1% TFA in H_2O; B = 80% ACN and 0.1% TFA in H_2O). The elution was monitored at 215 and 280 nm. To assess potential protein oligomerization, the purified lyophilized protein was diluted to 4 mg/mL concentration in H_2O, incubated for 30 min at room temperature and applied to Superdex 30 gel filtration column (1.6 x 60 cm) attached to a ÄKTA Purifier system. Protein was eluted using 50 mM Tris-HCl buffer (pH 7.4) at the flow rate of 1 mL/min. The elution was monitored at 215 and 280 nm.

Mass analysis - Perkin-Elmer Sciex API300 LC/MS/MS mass spectrometer (Thornton, Canada) was used to determine the precise masses and purity of the native protein as well as generated peptides. Ionspray, orifice and ring voltages were set at 4600 V, 50 V and 350 V, respectively. Nitrogen was used as curtain gas with a flow rate of 0.6 µL/min and as nebulizer gas with a pressure setting of 100 psi. The mass was determined by direct injection at a flow rate of 50 µL/min using the LC-10AD Shimadzu Liquid Chromatography pump as the solvent delivery system (50% ACN and 0.1% formic acid in H_2O). BioMultiview software was used to analyze mass spectra.

Unblocking and sequencing of the NH_2-terminal - *Pfu* pyroglutamate aminopeptidase digestion was performed to remove pyroglutamic acid (pGlu) residue which was blocking the NH_2-terminal of the protein. Enzymatic digestion was carried out in 50 mM sodium phosphate buffer pH 7.0 containing 10 mM DDT and 1 mM EDTA with 2 mU enzyme to 1 nmol protein ratio. The reaction was incubated for 10 h at 50 ºC, followed by NH_2-terminal sequencing by automated Edman degradation on a Perkin-Elmer Applied Biosystems 494 pulsed-liquid phase protein

sequencer (Procise) with an online 785A PTH-amino acid analyzer.

Peptide generation and protein sequencing - Lyophilized protein (500 µg) was dissolved in 500 µL of 0.13 M Tris-HCl, 1 mM EDTA, 6 M guanidine HCl, pH 8.5 and reduced with 10 µL of β-mercaptoethanol. This mixture was incubated at 37 ^{o}C for 2 h under N_2. Subsequently, 100 µL of alkylating reagent (4-vinyl pyridine) was added and the mixture incubated for another 2 h under N_2 at room temperature in the dark. The alkylated toxin mixture was immediately loaded onto a µRPC C2/C18 (10 µ, 120 Å, 2.1 x 100 mm) column attached to SMART Workstation (Amersham Pharmacia, Uppsala, Sweden). The column was washed for 30 min with buffer A followed by protein elution with a linear gradient of 0 to 50% solvent B (A = 0.1% TFA in H_2O; B = 80% ACN and 0.1% TFA in H_2O). Lyophilized pyridylethylated protein was then subjected to enzymatic digestion with Lys-C endopeptidase or trypsin. Protein (250 µg) was dissolved in 250 µL of enzymatic digestion buffer (50 mM Tris-HCl, 4 M urea, 5 mM EDTA pH 7.5) and proteases were added at a ratio of 1:50 (w/w). Cleavages were performed at 37 ºC for 16 h. The peptides generated were separated on a µRPC C2/C18 (10 µ, 120 Å, 2.1 x 100 mm) column attached to same chromatographic system using a linear gradient of 15 to 40% solvent B over an hour (A = 0.1% TFA in H_2O; B = 80% ACN and 0.1% TFA in H_2O). The flow rate was 200 µL/min. Eluted peptides were monitored at 215 nm, 254 nm and 280 nm. Amino acid sequence of the peptides was obtained by automated Edman degradation on an ABI Procise sequencer.

Total RNA isolation - Five days after milking, *B. dendrophila* specimen was sacrificed by an overdose of CO_2. The pair of venom glands was dissected and stored in RNAlater at -80 °C until use. Total RNA extraction was performed with rotor homogenizer and RNeasy mini kit. The amount of RNA was calculated according to 260 nm absorbance of the sample.

Reverse transcription - polymerase chain reaction (RT-PCR) - Based on the available amino acid sequence of the protein, the following degenerate primers were designed to obtain partial cDNA sequence: RT-forward 5'GCICCIGTRCARCAYTTIAC3' and RT-reverse 5'TGYTTIGCIGTIGGMCACAT 3'. One-step RT-PCR was carried out using 100 ng of total RNA and the following conditions: RT at 50 ºC for 30 min followed by activation of hot start *Taq* polymerase at 95 ºC for 15 min and 30 cycles of 3-step PCR (94 ºC for 1 min, 50 ºC for 1 min, 72 ºC for 1 min) followed by the final extension at 72 ºC for 10 min. PCR products were subjected to 1% agarose gel electrophoresis and visualized by ethidium bromide staining.

Cloning and sequencing of RT-PCR products - Amplification products were purified using PCR purification kit, ligated with pDrive vector and transformed by heat shock method into DH5α strain of competent *E. coli* cells. Selection of the transformants (blue/white colony screening) was performed on LB-agar plates containing 100 µg/mL ampicillin and supplemented with IPTG and X-gal. Sizes of the inserts were estimated by *Eco*RI digestion followed by 1% agarose gel electrophoresis and ethidium bromide visualization. All sequencing reactions were carried out on the ABI PRISM® 3100 automated DNA sequencer, using the BigDye terminator cycle sequencing ready reaction kit according to the manufacturer's instructions. All clones were sequenced in both directions using T7 and SP6 sequencing primers.

Sequences analysis - Sequence analysis was carried out using the BLAST program at the National Center for Biotechnology Information website (www.ncbi.nlm.nih.gov) and ExPASy proteomics tools at www.expasy.ch. Sequence alignments were carried out using the ClustalW program at www.ebi.ac.uk or DNAMAN version 4.15 (Lynnon Biosoft).

Chemical synthesis - Chemical synthesis and assembly of protein was performed on an Applied Biosystems 431 peptide synthesizer using a modified version of the Applied Biosystems standard 0.1 mmol small-scale program (26) with HOAT as the coupling reagent and *N*-methyl pyrrolidone as the solvent. Fmoc-protected amino acids were used with the following side chain protections: *t*-butyl ester (Glu, Asp), *t*-butyl ether (Ser, Thr, Tyr), *t*-butylcarbonyl (Lys), trityl (Cys,

His, Asn, Gln), 2,2,5,7,8-pentamethyl-chromane-6-sulfonyl (Arg), and *t*-butyloxycarbonyl (Trp). The toxin was assembled on an Fmoc-Asp(OtBu)-Wang resin (loading, 0.55 mmol/g) (27). The synthesis was performed using the improved software, armed with UV deprotection step monitoring, which in the case of deprotection failure automatically extends the deprotection and coupling time for the particular amino acid (28). After each coupling, the resin was acetylated by a mixture of 5% acetic anhydride and 6% 2,4,6-collidine in dimethylformamide. At the end of the synthesis, the peptide-resin was treated with a mixture of trifluoroacetic acid (90%), tri-isopropylsilane (5%) and distilled water (5%) in order to cleave the peptide from the resin and to remove the protecting groups from amino acid side chains. After 2 h of incubation at room temperature with constant mixing, the crude material was filtered and precipitated in cold *tert*-butyl methyloxide. Precipitates were washed three times with *tert*-butyl methyloxide followed by centrifugation at 1700 g and re-suspension in 10% acetic acid. Lyophilized crude synthetic toxin was then reduced with molar excess of TCEP for at least 30 min (to reduce incorrectly formed disulphide bonds) and purified by reversed phase HPLC using a Discovery®BIO Wide Pore C5 (5 µ, 300 Å, 10 x 250 mm) with a gradient of 40 to 60% of solvent B over 40 min (A = 0.1% TFA in H_2O; B = 60% acetonitrile and 0.1% TFA in H_2O). The flow rate was 3 mL/min and the elution was followed at 215 and 280 nm.

Purification and refolding of synthetic toxin - The reduced synthetic peptide was dissolved in 200 µL distilled water to evaluate protein concentration based on absorbance at 278 nm. It was then diluted with the refolding buffer (0.1 M Tris-HCl pH 7.8, 0.5 M guanidium chloride, GSH and GSSH in molar ratio of 10:1) to a concentration of 0.05 mg/mL and incubated 2-4 days in 4 ºC. The mixture was acidified with 20% TFA and purified on the Discovery®BIO Wide Pore C5 column with a gradient of 30 to 50% solvent B over 40 min (A = 0.1% TFA in H_2O; B = 60% acetonitrile and 0.1% TFA in H_2O). The flow rate was 3 mL/min and the elution was followed at 215 and 280 nm. The synthetic and native toxins were compared by co-elution profile and circular dichroism spectra.

In vivo *toxicity test* - The native protein was injected intraperitoneally in male Swiss-Webster mice (19 ± 2 g) at doses of 0.1 mg/kg, 1 mg/kg, 10 mg/kg and 20 mg/kg (n = 2). All doses were made up to a volume of 200 µL in saline. The same volume of normal saline was injected intraperitoneally to control animals. Mice were observed for 6-8 h and sacrificed after 24 h to perform the autopsy. Intracerebroventricular injections of the protein (0.1 mg/kg, 1 mg/kg, 10 mg/kg in 5 µL of saline, n = 2 per dose) and control saline (5 µL, n = 2) were performed in 19 ± 2 g mice using a fine capillary Hamilton micro-syringe. Animals were sacrificed for autopsy after 5 h of observation.

Chick biventer cervicis muscle (CBCM) preparations - A pair of CBCM was isolated from 6-10 day old chicks and mounted in an 8 mL organ bath (29) containing Krebs solution continuously aerated with 5% CO_2 in O_2. The temperature of the organ bath was maintained at 35 °C. The resting tension of the isolated tissue was adjusted to ~1 g. Electrical field stimulation was carried out through platinum ring electrodes using a Grass stimulator S88 (Grass Instruments, MA, USA). The data was transferred via a force displacement transducer (Model FT03, Grass Instruments, Quincey, MA, USA) and was recorded using a Power Lab 6 system (ADInstruments, Bella Vista, NSW, Australia). Maximal twitch responses of the muscle were elicited indirectly via stimulating the motor nerve by applying electrical field of 7-10 V potential difference, at the frequency of 0.2 Hz in supramaximal rectangular pulses of 0.1 ms duration. The preparation was equilibrated for 30-50 min before the beginning of an experiment, with changes of Krebs solution at 10 min intervals. To ensure selective stimulation of the motor nerve, d-turbocurarine (10 µM) was added, with subsequent abolition of twitches, which were then re-established after a thorough wash. At appropriate intervals, submaximal control contractures to exogenously applied 300 µM acetylcholine (ACh), 8 µM carbachol (Cc) or 30 mM potassium chloride (KCl) were obtained in the absence of an electrical field. The contact time for these agonistic drugs was 30, 90 and 60 sec, respectively, followed by a wash with about 100 mL of fresh Krebs solution. The electrical stimulation was then recommenced and after

stabilization of twitch height, the effects of various concentrations of denmotoxin (0.1 μg/mL - 100 μg/mL; 11.8 nM - 11.8 μM; n = 5), α-bungarotoxin (0.1 nM - 0.5 μM; n = 3) or vehicle was investigated. The neuromuscular block is expressed as a percentage of original twitch height in the absence of toxin. Dose-response representing % of block after 30 min of CBCM exposure to the respective toxins was plotted. Each preparation was exposed to only one dose of toxin, and both muscles from the same specimen were used to test two different doses. The reversibility of the inhibitory effect of the toxin on twitches was assessed by the replacement of Krebs solution in the organ bath at 10 min intervals combined with slow drip-wash over 180 min. The effect of neostigmine (10 μM) on the reversal of neuromuscular blockage was also examined.

Mouse hemidiaphragm muscle (MHD) preparations - MHD with the associated phrenic nerve was isolated as described by Bulbring (30) and mounted in a 5.5 mL organ bath. Indirect stimulation was performed at a frequency of 0.2 Hz in rectangular pulses of 0.2 ms duration with supra-maximal voltage of 7-10 V. Positive control was performed with α-bungarotoxin (10 nM, 50 nM, 100 nM; n = 3). The partial dose-response curves for denmotoxin was determined (doses: 117.5 nM, 1.175 μM, 11.75 μM; n = 3 and 2.35 μM, 5.88 μM; n = 1). In control experiments, the effect of uninterrupted nerve stimulation of MHD was assessed. Also the recovery of twitches was assessed by washing with Krebs solution overflow followed by slow drip-wash. In order to eliminate batch to batch variations of the protein during the experiments all CBCM and MHD experiment were performed using same protein stock solution. Data are expressed as mean ± standard error of mean (S.E.M.). Data were analysed and fitted using Fig.P software version 2.98 (Fig.P Software Corporation, Durham, NC, USA).

Crystallization - Lyophilized protein was re-suspended in 50 mM Na acetate, pH 5.5, containing 0.02% sodium azide, washed four times to remove salts and re-concentrated to 10 mg/mL using ultrafiltration with 5 kDa cut-off Amicon filter (Millipore, Billerica, MA, USA). Crystallization experiments were carried out using the sitting drop vapor diffusion method at 291 K (18 °C). In initial crystallization experiments Hampton Research screens I and II were used and setups contained 1 μL of protein and 1 μL of the reservoir solution. Final conditions were optimized by seeding to bypass spontaneous nucleation and hence control the number of crystals and improve their growth. Crystals for diffraction were kept in cryoprotectant solution containing 1.5 M $LiSO_4$ with 25 mM imidazole, pH 8.0 and flash-frozen in liquid ethane.

X-ray diffraction data collection, structure determination and refinement - The crystal diffraction was performed on beam line ID-29 at the European Synchrotron Radiation Facility (ESRF, Grenoble, France). The data was processed using the HKL package (31) and the structure was solved using molecular replacement method. Different search models were tried out to find the proper rotation and translation solution. To choose the best model for molecular replacement method FASTA search was conducted using protein sequence against the PDB database. The closest match found was the crystal structure of neurotoxin-1 from *Naja naja oxiana* (1NTN). Based on this molecule, the denmotoxin search model was built by residue replacement. Several other homology models were tried in a different resolution range, but no solution could be found. Finally, the proper solution was found using native data and a search model built based on irditoxin (PDB #2H7Z) with partial deletions of loops regions. The programs: MOLREP (32), Refmac (33), CNS (34) and PROCHECK (35) were used to solve, refine and analyze the structure.

RESULTS

Identification and purification of toxin - LC/MS profile revealed that the most abundant proteins in crude venom *of B. dendrophila* have molecular masses ~8-10 kDa (25). Among them, we have identified one major component with mass of ~8508 Da (Fig. 1A). This protein was purified to homogeneity by consecutive cation exchange chromatography (Fig. 1B) and RP-HPLC (Fig. 1C). On a UNO S-6 column *B. dendrophila* venom was separated into ten fractions (Fig. 1B). Each peak was then subjected to RP-HPLC and the individual fractions from RP-HPLC were assessed

using ESI/MS (data not shown). The peak 2 from cation exchange column (Fig. 1B) contained the protein of interest (Fig. 1C). The protein was found to be homogenous with the precise molecular mass of 8507.92 ± 0.30 Da as determined by ESI mass spectrometry (Fig. 1D). The purification yielded approximately 5 mg of the toxin from 100 mg of crude venom. The protein was confirmed to be a monomer using gel filtration chromatography (Fig. 1E) as only one peak eluted at the retention time of 73 min corresponding to ~8 kDa (monomeric) mass. We named this protein "denmotoxin" (*B. dendrophila* monomeric toxin).

Determination and analysis of amino acid sequence - The first attempt to obtain the amino terminal sequence of denmotoxin by Edman degradation failed, as the toxin was NH_2-terminally blocked by pyroglutamic acid. Pyroglutamate aminopeptidase was used to remove the blocking group. NH_2-terminal sequencing of the unblocked protein resulted in identification of the first 20 residues (Fig. 1F). Further sequence data was obtained by the generation and sequencing of peptides following digestion of the pyridylethylated protein with lysyl endopeptidase and trypsin (Fig. 1F). Peptides from respective digests were separated by RP-HPLC (data not shown) and subjected to automated Edman degradation. More than 90% of the sequence (except the WAVK fragment) was determined by protein sequencing (Fig. 1F). Based on the available amino acid sequence, degenerate primers were designed to fish out the missing fragment using RT-PCR and to determine the complete sequence of the toxin. Using this strategy, we were able to identify unequivocally all residues of denmotoxin (GenBank # DQ366293). The protein possesses 77 amino acid residues, including 10 cysteines (Fig. 2). The calculated mass of denmotoxin, with the observed pyroglutamation and five disulphide bridges, is 8507.8 Da, nearly identical with the observed molecular mass (8507.92 ± 0.30 Da) estimated by ESI mass spectrometry (Fig. 1D). The multiple sequence alignment, in particular, cysteines' arrangement (Fig. 2) indicates that denmotoxin belongs to the class of non-conventional 3FTXs (3). Denmotoxin differs structurally from elapid 3FTXs in having seven additional residues at its NH_2-terminus, which is blocked by a pyroglutamic acid residue (Fig. 2). In this respect it is similar to 3FTXs isolated from colubrid venoms, such as α-colubritoxin (18) and boigatoxin-A (25). Denmotoxin shares about 50% identity with α-colubritoxin, but it shows less than 30% identity with elapid 3FTXs (Fig. 2) and only ~15-20% identity, if the five disulphide bridges, which contribute significantly to the percentage of identity, are excluded.

Synthesis and characterization of synthetic denmotoxin - The investigation of colubrid venom components is severely limited because of the tedious extraction procedure and low venom yields (23). Therefore, we chemically assembled denmotoxin by solid phase peptide synthesis. The yield from peptide synthesis was about 30% based on deprotection monitoring at 301 nm. Reduced crude peptide was purified from contaminating side-products on RP-HPLC (Fig. 3A). The major peak contained a homogenous peptide with a molecular mass 8517.38 ± 0.44 Da as assessed by ESI-MS (Fig. 3B) precisely matching the calculated mass for the reduced form of denmotoxin (8517.8 Da). This reduced synthetic denmotoxin was subjected to glutathione-mediated oxidation followed by acidification and RP-HPLC purification. The oxidized peptide eluted as a major component about 10 min earlier than the reduced form (data not shown) and therefore for greater purification, the gradient was modified (Fig. 3C). The synthetic, oxidized denmotoxin was homogenous, with a molecular mass of 8507.70 ± 0.22 Da (Fig. 3D), which exactly matched the mass of native protein. Further, the native and synthetic proteins were shown to be identical based on co-elution profiles on RP-HPLC (Fig. 3E) and CD spectroscopy analysis (data not shown). To compare the pharmacological action of the synthetic and native denmotoxin, we tested both preparations in chick biventer experiments. Our results indicate that they displayed identical physicochemical and pharmacological properties.

Species-specific neuromuscular blockage - Denmotoxin caused time- and concentration-dependent blockage of the twitch responses of indirectly stimulated CBCM preparation (Fig. 4). It also completely inhibited contractile responses of the exogenously applied nicotinic agonists

(ACh and Cc) (Fig. 4A), but did not show any inhibition of 50 mM KCl (Fig. 4A) or direct twitches in the preparation (data not shown). Thus denmotoxin acts as a postsynaptic neurotoxin. The neuromuscular blockage was virtually irreversible and sustained for up to 180 min without spontaneous reversal despite washing the organ bath with Kreb's solution (Fig. 4A).The addition of neostigmine (10 μM) to tissues treated with 0.24 μM of denmotoxin was not able to restore partially diminished nerve-evoked twitches (data not shown). Similarly, α-bungarotoxin produced pseudo-irreversible blockage, neither affected by wash nor by the addition of neostigmine (data not shown). However, α-bungarotoxin was 10 fold more potent than denmotoxin (Fig. 4C).

In contrast, denmotoxin showed a very weak effect on neuromuscular transmission in mouse hemidiaphragm. The blockage produced by denmotoxin in MHD was up to 100-fold smaller than that produced in CBCM and denmotoxin was not able to produce complete blockage of indirectly stimulated twitches up to 11.76 μM (Fig 4C). Moreover, unlike irreversible denmotoxin-induced blockage in CBCM, that in MHD was rapidly reversed by washing (Fig. 4B). In contrast, the positive control (α-bungarotoxin) used in MHD experiments virtually irreversibly blocked with similar dose-response curve as in CBCM experiments (Fig. 4C). Thus, denmotoxin induces partial and reversible block of neurotransmission in MHD. In agreement with this finding, we observed no paralysis or other biological effects in mice after intraperitonial or intracerebroventrical injection of the toxin, up to 20 and 10 mg/kg, respectively. Taken together, these results indicate a clear species-dependent toxicity and susceptibility of chick muscle nAChR to denmotoxin.

Three-dimensional structure - We determined the three-dimensional structure of denmotoxin, a unique 3FTX with an unusually long NH_2-terminal segment, by crystallization and X-ray diffraction methods. The most suitable crystals were obtained in a solution containing 1.2 M $NaKPO_4$ (NaH_2PO_4 + K_2HPO_4), pH 7. They belong to monoclinic space group C2 with two molecules of denmotoxin by asymmetric unit. The crystal diffracted to 1.7 Å on a synchrotron beam line and the structure of denmotoxin was solved using molecular replacement method. The model was refined to 1.9 Å and Procheck program confirmed the standard stereochemistry. Statistics for data collection and refinement are shown in Table I. Coordinates of the structure have been deposited in the Protein Data Bank with the code number PDB #**2H5F**. The electron density maps were excellent for the whole molecule except for the three first residues at the NH_2-terminal and the tip of the central loop suggesting high flexibility in these regions. 284 water molecules and four phosphate, two potassium and two sodium ions from mother liquor ($NaKPO_4$) were also identified in these electron density maps. Two phosphate ions are located near Arg55 of respective molecules, while two others (near Arg26) seem to stabilize intermolecular interactions and contribute to crystallographic dimer formation. Denmotoxin's structure is similar to other 3FTXs (Fig. 5B). Erabutoxin-b (*Laticauda semifaciata*), bucandin (*Bungarus candidus*), toxin-b (*Ophiophagus hannah*) and toxin-γ (*Naja nigricollis*) show the closest match as shown by Dali search algorithm (36). Denmotoxin consists of three polypeptide loops, with four disulphide bridges holding the molecule at the central core, and a fifth disulphide bridge located at the tip of the first loop (Fig. 5A) as is also found in elapid non-conventional toxins (3). The major element of secondary structure is a triple-stranded antiparallel β-sheet, consisting of two strands from the second loop and one strand from the third loop. Despite being a representative of 3FTX family, denmotoxin displays unique features like the twisted tip of the central loop, which originates from the kink of Pro40 (Fig. 5, A and B). The unusual long NH_2-terminal of seven residues is clearly unstructured and probably flipping above the core of the molecule (Fig. 5, A and B), the first three NH_2-terminal residues being even not seen in electron density map. The surface charge density of denmotoxin is relatively uneven and the electrostatic potential of the tip of the central loop is negative, unlike other neurotoxins of the 3FTX family (Fig. 5C). The crystal structure of denmotoxin is the first high resolution structure of a colubrid 3FTX, and it provides a platform for further investigations to decipher the basis of denmotoxin interactions with the target receptor.

DISCUSSION

Snake venoms are a rich source of pharmacologically active proteins and polypeptides. A number of toxins have provided excellent research tools used to decipher molecular details of physiological processes, and several have led to the development of novel therapeutic agents (37;38). Among snake venoms, colubrid venoms are the least studied because of the lack of commercial sources, the difficulty in extraction procedures and the low yield of venoms (22), and thus the chemistry of venoms from this large group of snakes is poorly understood. As colubrids have a distinct evolutionary lineage, they are expected to provide interesting new groups of protein toxins. Indeed in the present study, we isolated and characterized a novel colubrid toxin, denmotoxin from *B. dendrophila* venom. The mature protein has 77 amino acid residues, including 10 cysteines, and belongs to the non-conventional class of the 3FTX family. However, it shows low sequence identity with other 3FTXs and has an extended NH_2-terminal segment which appears to be unique to colubrid venoms. Pharmacological studies reveal that denmotoxin is a taxon-specific postsynaptic neurotoxin. High resolution crystal structure shows that it structurally resembles to other elapid 3FTXs, but it also possesses the unusually long NH_2-terminal flipping above the core of molecule and a twisted central loop negatively charged at its tip. It is the first description of pharmacological and structural properties of a colubrid toxin.

In an attempt to obtain denmotoxin in larger quantities, we synthesized it by solid phase peptide synthesis using Fmoc chemistry. The synthesis of denmotoxin without using chemical ligation was challenging, as the protein is a 77 amino acid residues long, β-sheeted polypeptide, rich in disulphide bridges and therefore prone to aggregation and incorrect disulphide formation. To enhance the assembly, UV monitoring of deprotection and automatic extension of the deprotection time to 20 min and the coupling time to 30 min was used, when the deprotection was not sufficient after 2 successive 3 min deprotections. Using this method, the overall yield of synthesis was about 30%, much higher than often obtained with peptides of this length. Peptide synthesis allowed us to obtain considerable quantities of the toxin without resorting to traditional purification methods. It should be emphasized that the oxidized synthetic peptide has all biochemical characteristics of the natural toxin and was virtually indistinguishable from native toxin in organ bath experiments. These results ruled out the possibility that activity of native denmotoxin may be due to potential contaminants from the crude venom as was shown in the case of κ-bungarotoxin containing a minor impurity of potent α-bungarotoxin (39). In addition, an Fmoc-based chemical approach might be useful for future mutagenesis studies of denmotoxin.

Venoms from snakes of the genus *Boiga* exhibit postsynaptic neurotoxicity. For example, *Boiga blandingi* venom irreversibly inhibits motor end-plate potential in frog nerve-muscle (40), *Boiga irregularis* venom shows competitive binding with cobrotoxin to nAChRs in an enzyme-linked immunoassay (41) and partially purified components of *B. dendrophila* venom (approximately 11 and 12 kDa) bind to *Torpedo marmorata* AChRs (42). Recently, *B. dendrophila* venom (43;44) and a toxin isolated from this venom, boigatoxin-A (Fig. 1A) have been shown to block irreversibly twitches of chick biventer cervicis muscle preparations. Boigatoxin-A (45) has a molecular mass of 8769 Da and its NH_2-terminal 47 residues show 78% identity to denmotoxin. Similar to boigatoxin-A, denmotoxin exhibits a postsynaptic neurotoxic effect in chick biventer cervicis muscle. Denmotoxin inhibited the indirect twitches and exogenous agonist responses, indicating its postsynaptic effects (Fig. 4). However, it exhibited neurotoxic effects differently in mouse hemidiaphragm experiments, being about 100 fold weaker, readily-reversibly blocking the indirectly stimulated twitches, a finding which explains why denmotoxin neither paralyzes nor shows any other effects in mice after intraperitonal injection even at 20 mg/kg. This data strongly suggest that denmotoxin is able to discriminate between the peripheral nAChRs from two species. Boigatoxin-A was tested only on chick but not on mice neuromuscular junctions and hence it is not clear whether it would also exhibit similar species-specify. Species-specific neurotoxicity is known for colubrid venoms. For example, neurotoxicity of *Philodryas*

patagoniensis (46;47) venom was more specific towards pigeons than to guinea pigs, rabbits and frogs. Also, both the crude venom and partially purified venom components of *P. olfersii* showed postsynaptic neurotoxicity on CBCM while MHD preparations were unaffected (48). Recently it was also demonstrated that the venom of *Boiga irregularis* (49) displays taxa-specific toxicity, and denmotoxin is the first well-characterized venom component which shows species-specific effects. It is interesting to note that *B. dendrophila* preys primarily on birds (21). As there is a correlation between toxin specificity and a snake's diet (49), the major venom components in *B. dendrophila* venom have probably evolved to target birds. Denmotoxin may be one such toxin targeted to affect birds. Thus care must be taken when studying toxicity of such venoms, as LD_{50} studies conducted using mouse models only may not truly reflect the toxic potency of the venom components (22).

Denmotoxin shares less than 30% sequence identity with other 3FTXs (except α-colubritoxin), but it retains the residues involved in maintaining the three-finger fold. Much of this sequence identity is due to conserved disulphide bridges and several structurally important residues. Denmotoxin possesses all four conserved disulphide bridges located in the core region, reduction of which has been shown to disturb the overall conformation and result in the total loss of function (50). In addition, denmotoxin has most of the invariant residues that are important for the proper folding and the three-dimensional structure. Tyr25 (all numberings are according to erabutoxin-a) has been shown to be a highly conserved and structurally important residue (51;52). Antil et al. (53) have shown that mutation of its equivalent in α-cobratoxin (Tyr21Ala) prevents proper folding of the protein. Moreover, Tyr21 was shown to stabilize the anti-parallel β-sheet structure (54). Denmotoxin also possesses Tyr35 with the side chain oriented exactly in the same way, although in most non-conventional toxins this tyrosine is replaced by a homologous Phe25. Another residue important for maintaining spatial conformation is Gly40, placed opposite of Tyr25 to accommodate the bulky side chain. The equivalent Gly is present as Gly52 in denmotoxin. Also, Pro44 has been shown to be structurally important (51), and it is represented by Pro58 in denmotoxin. The presence of these structurally important residues in denmotoxin results in the retention of the characteristic three-finger fold as is apparent from the crystal structure (Fig. 5B).

The functionally important residues involved in receptor binding in short- and long-chain neurotoxins have been studied in detail (55-58). Moreover, recently determined crystal structure of α-cobratoxin complexed with acetylcholine binding protein (AChBP) illustrates the critical residues involved in toxin-receptor interactions (59). Erabutoxin-a and α-cobratoxin interact with *Torpedo* $\alpha_1\beta\gamma\delta$ using common core of residues: Lys27/Lys23; Trp29/Trp25; Asp31/Asp27; Phe32/Phe29; Arg33/Arg33, and Lys47/Lys49. The first five of the above residues are replaced by unconserved residues in denmotoxin: Leu37; Lys39; Gly44; Glu42; and Asp41, respectively. Most importantly, Arg33 is replaced by negatively charged aspartic acid at the tip of loop II. Arg33 is one of the most critical residues and its replacement by glutamic acid results in over 300 and 750 folds affinity loss of binding in erabutoxin-a (60;61) and α-cobratoxin (53), respectively. Apart from common core residues, erabutoxin-a utilizes specific determinants crucial for *Torpedo* receptor recognition: Gln7, Ser8, Gln10, Ile36 and Glu38. These residues correspond in denmotoxin to Asn14, Arg15, Ser19, Trp48 and Val50, respectively. It is not clear how denmotoxin retains significant neurotoxicity (only a 10-fold loss compared to α-bungarotoxin) although most of the functional residues are replaced. It is possible that denmotoxin binds to nAChR utilizing other residues which are yet to be identified.

Some of 3FTXs bind to their receptors virtually irreversibly whereas others exhibit reversible binding (18;62;63), and the molecular determinants which contribute to reversibility are not known. However, it was reported that the mutation of a single amino acid residue (Phe38 to Ile) in the muscarinic 3FTX m1-Toxin1 (*Dendroaspis angusticeps*) changes toxin binding to M_1 muscarinic receptor from irreversible to completely reversible (64). As shown here, the neuromuscular block of chick nerve-muscle junction by denmotoxin is irreversible. α-

Colubritoxin (from *Coelognathus radiatus* venom), which shows about 50% sequence identity to denmotoxin, exhibits a potent postsynaptic effect and completely inhibits indirect twitches in CBCM in 30 min (1 μM), but this block is reversible (18). Structure-function relationships of these two toxins may help us delineate the residues involved in their reversible/ irreversible binding. The physiological relevance of such reversibility of binding is not clear but may result from selection for specific structural variants of 3FTXs with taxa-specific effects (49).

During the evolution of nAChR, residues critical for α-neurotoxin binding (65;66) are highly conserved in various taxa (from fishes to mammals), but in resistant organisms, this region is often significantly modified. Some of the species-specific susceptibility/resistance to postsynaptic neurotoxins are correlated with a substitution of residues leading to additional *N*-glycosylation site near the ligand binding site in the nAChR (67;68). A functional result of this modification is that the motor endplate nAChR of many snakes and mammals such as the mongoose are much less sensitive to postsynaptic neurotoxins (69;70). Comparative sequence analysis of nAChR from mouse, mongoose and snake shows a mutation of mouse Trp187Asn in mongoose (67) and Phe189Asn in snake (68). These additional *N*-glycosylation sites confer a barrier to the toxin, allowing an access for small ligands like acetylcholine. We compared the amino acid sequences of chick (α - P09479, β - P16005, γ - P02713, δ - P02717) and mouse (α - NP_031415, β - P09690, γ - P04760, δ - P02716) $\alpha_1\beta\gamma\delta$ nAChR. They show high sequence identity, overall as well as within functional loops. There is no difference in *N*-glycosylation pattern between chick and mouse receptor. Thus, reversibility and resistance of mouse nAChRs to denmotoxin does not appear to be related to the differences in glycosylation. As the tip of the central loop of denmotoxin is negatively charged, in contrast to the positively charged tip in postsynaptic neurotoxins (Asp41 in denmotoxin versus Arg33 in erabutoxin-a and α-cobratoxin), we focused on substitutions leading to charge changes in the regions with the close proximity to the toxin binding site in the mouse and chick $\alpha_1\beta\gamma\delta$ nAChRs. Functional loops A and B from the α-subunit and loops F from γ and δ subunits are identical in both species (Fig. 6A). In loop C (α-subunit), loops D and E (γ and δ subunits) there are several amino acid replacements, when compare the sequences of both nAChRs (Fig. 6A), which may contribute to species-dependent receptor susceptibility to denmotoxin. However, in these segments none of the substitutions led to an increase in positive charge in chick receptor as compared to that of mice, which could explain the taxon-specific binding of denmotoxin. Recently, AChBP from *Lymnaea stagnalis*, a homologue of the N-terminal ligand-binding domain of nAChRs, has been co-crystallized with α-cobratoxin (PDB #1UX2) (59). The complex structure reveals receptor-toxin interactions. There is an unstructured region between β8 and β9 (Fig. 6, B and C), which is involved in the interaction. This segment is considered to be equivalent to the complimentary face of the γ and δ subunits of muscle nAChRs. Unlike in mouse $\alpha_1\beta\gamma\delta$, there is an Arg193 in δ subunit of the chick $\alpha_1\beta\gamma\delta$ nAChR in this region, just in front of functional loop F (Fig. 6C). This Arg193 may contribute towards electrostatic interactions with denmotoxin Asp41, causing an enhanced and irreversible binding of the toxin to chick $\alpha_1\beta\gamma\delta$ nAChR. Thus, Arg193 of chick δ subunit may explain the observed species-specificity. However, toxin-receptor interactions are likely complex and further studies (e.g. double cycle mutants experiments with chicken and mouse $\alpha_1\beta\gamma\delta$ nAChRs) are needed to elucidate the relative importance of residue substitutions.

CONCLUSIONS

We have identified, purified and characterized a novel toxin, denmotoxin, from the venom of the colubrid snake *Boiga dendrophila.* It exhibits taxon-specific postsynaptic neuromuscular blockade; it potently and irreversibly blocks chick neuromuscular transmission, but weakly and reversibly blocks mouse neuromuscular transmission. Crystallographic determination of the three-dimensional structure of this unique 3FTX, which possesses an NH_2-terminal extension, demonstrates that the characteristic structural motif of the 3FTXs is conserved. The structural and functional characterizations of this colubrid non-conventional 3FTX will provide the

foundation for a better understanding of species-specificity and reversibility of postsynaptic neurotoxins.

ACKNOWLEDGMENTS

We thank Shoon Mei Leng for her invaluable help, assistance and technical advice during organ bath experiments, William H. Heyborne for assistance with venom extractions and Dr. S. Jayaraman for help in final structure refinement. This work was supported by grant from the Biomedical Research Council, Agency for Science, Technology and Research, Singapore.

REFERENCES

1. Endo, T. and Tamiya, N. (1987) *Pharmacol.Ther.* **34,** 403-451
2. Kini, R. M. (2002) *Clin.Exp.Pharmacol.Physiol* **29,** 815-822
3. Nirthanan, S., Gopalakrishnakone, P., Gwee, M. C., Khoo, H. E., and Kini, R. M. (2003) *Toxicon* **41,** 397-407
4. Servent, D. and Menez, A. (2001) Snake neurotoxins that interact with nicotine acetylcholine receptors. *Handbook of Neurotoxicology*,
5. Tsetlin, V. (1999) *Eur.J.Biochem.* **264,** 281-286
6. Ricciardi, A., Le Du, M. H., Khayati, M., Dajas, F., Boulain, J. C., Menez, A., and Ducancel, F. (2000) *J.Biol.Chem.* **275,** 18302-18310
7. Ohno, M., Menez, R., Ogawa, T., Danse, J. M., Shimohigashi, Y., Fromen, C., Ducancel, F., Zinn-Justin, S., Le Du, M. H., Boulain, J. C., Tamiya, T., and Menez, A. (1998) *Prog.Nucleic Acid Res.Mol.Biol.* **59,** 307-364
8. Potter, L. T. (2001) *Life Sci.* **68,** 2541-2547
9. Yasuda, O., Morimoto, S., Jiang, B., Kuroda, H., Kimura, T., Sakakibara, S., Fukuo, K., Chen, S., Tamatani, M., and Ogihara, T. (1994) *Artery* **21,** 287-302
10. De Weille, J. R., Schweitz, H., Maes, P., Tartar, A., and Lazdunski, M. (1991) *Proc.Natl.Acad.Sci.U.S.A* **88,** 2437-2440
11. McDowell, R. S., Dennis, M. S., Louie, A., Shuster, M., Mulkerrin, M. G., and Lazarus, R. A. (1992) *Biochemistry* **31,** 4766-4772
12. Williams, J. A., Lu, X., Rahman, S., Keating, C., and Kakkar, V. (1993) *Biochem.Soc.Trans.* **21,** 73S
13. Wu, P. L., Lee, S. C., Chuang, C. C., Mori, S., Akakura, N., Wu, W. G., and Takada, Y. (2006) *J.Biol.Chem.* **281,** 7937-7945
14. Karlsson, E., Mbugua, P. M., and Rodriguez-Ithurralde, D. (1984) *J.Physiol (Paris)* **79,** 232-240
15. Kumar, T. K., Jayaraman, G., Lee, C. S., Arunkumar, A. I., Sivaraman, T., Samuel, D., and Yu, C. (1997) *J.Biomol.Struct.Dyn.* **15,** 431-463
16. Banerjee, Y., Mizuguchi, J., Iwanaga, S., and Kini, R. M. (2005) *J.Biol.Chem.*
17. Chang, C. C. (1999) *J.Biomed.Sci.* **6,** 368-375
18. Fry, B. G., Lumsden, N. G., Wuster, W., Wickramaratna, J. C., Hodgson, W. C., and Kini, R. M. (2003) *J.Mol.Evol.* **57,** 446-452
19. Vidal, N. and Hedges, S. B. (2002) *C.R.Biol.* **325,** 987-995
20. Vidal, N. and Hedges, S. B. (2005) *C.R.Biol.* **328,** 1000-1008
21. Hill, R. E. and Mackessy, S. P. (2000) *Toxicon* **38,** 1663-1687
22. Mackessy, S. P. (2002) *J.Toxicol.- Toxin Reviews* **21,** 43-83
23. Hill, R. E. and Mackessy, S. P. (1997) *Toxicon* **35,** 671-678

24. Chang, C. C. and Lee, C. Y. (1963) *Arch.Int.Pharmacodyn.Ther.* **144,** 241-257
25. Fry, B. G., Wuster, W., Ryan Ramjan, S. F., Jackson, T., Martelli, P., and Kini, R. M. (2003) *Rapid Commun.Mass Spectrom.* **17,** 2047-2062
26. Mourier, G., Servent, D., Zinn-Justin, S., and Menez, A. (2000) *Protein Eng* **13,** 217-225
27. Wang, S. S. (1973) *J.Am.Chem.Soc.* **95,** 1328-1333
28. Mourier, G., Dutertre, S., Fruchart-Gaillard, C., Menez, A., and Servent, D. (2003) *Mol.Pharmacol.* **63,** 26-35
29. Gilsborg, B. L. and Warriner, J. (1960) *Br.J.Pharmacol.Chemother.* **15,** 410-411
30. Bulbring, E. (1997) *Br.J.Pharmacol.* **120,** 3-26
31. Otwinowski, Z. and Minor, W. (1997) Macromolecular Crystallography, part A: Processing of X-ray Diffraction Data Collected in Oscillation Mode. In Carter, C. W. Jr. and Sweet, R. M., editors. *Methods in Enzymology*, Academic Press,
32. Vagin, A. and Teplyakov, A. (1997) *Journal of Applied Crystallography* **30,** 1022-1025
33. Murshudov, G. N., Vagin, A. A., and Dodson, E. J. (1997) *Acta Crystallogr.D.Biol.Crystallogr.* **53,** 240-255
34. Brunger, A. T., Adams, P. D., Clore, G. M., DeLano, W. L., Gros, P., Grosse-Kunstleve, R. W., Jiang, J. S., Kuszewski, J., Nilges, M., Pannu, N. S., Read, R. J., Rice, L. M., Simonson, T., and Warren, G. L. (1998) *Acta Crystallogr.D.Biol.Crystallogr.* **54 (Pt 5),** 905-921
35. Laskowski, R. A., MacArthur, M. W., Moss, D. S., and Thornton, J. M. (1993) *Journal of Applied Crystallography* **26,** 283
36. Holm, L. and Sander, C. (1995) *Trends Biochem.Sci.* **20,** 478-480
37. Lewis, R. J. and Garcia, M. L. (2003) *Nat.Rev.Drug Discov.* **2,** 790-802
38. Smith, C. G. and Vane, J. R. (2003) *FASEB J.* **17,** 788-789
39. Fiordalisi, J. J., al Rabiee, R., Chiappinelli, V. A., and Grant, G. A. (1994) *Biochemistry* **33,** 12962-12967
40. Levinson, S. R., Evans, M. H., and Groves, F. (1976) *Toxicon* **14,** 307-312
41. Weinstein, S. A., Chiszar, D., Bell, R. C., and Smith, L. A. (1991) *Toxicon* **29,** 401-407
42. Broaders, M., Faro, C., and Ryan, M. F. (1999) *J.Nat.Toxins.* **8,** 155-166
43. Lumsden, N. G., Fry, B. G., Kini, R. M., and Hodgson, W. C. (2004) *Toxicon* **43,** 819-827
44. Lumsden, N. G., Fry, B. G., Ventura, S., Kini, R. M., and Hodgson, W. C. (2004) *Auton.Autacoid.Pharmacol.* **24,** 107-113
45. Lumsden, N. G., Fry, B. G., Ventura, S., Kini, R. M., and Hodgson, W. C. (2005) *Toxicon* **45,** 329-334
46. Brazil, V. and Vellard, J. (1926) *Mem.Inst.Butantan* **3,** 301-325
47. Martins, N. (1917) *Col.Trab.Inst.Butantan 1907-1917* **1,** 427-496
48. Prado-Franceschi, J., Hyslop, S., Cogo, J. C., Andrade, A. L., Assakura, M., Cruz-Hofling, M. A., and Rodrigues-Simioni, L. (1996) *Toxicon* **34,** 459-466
49. Mackessy, S. P., Sixberry, N. M., Heyborne, W. H., and Fritts, T. (2006) *Toxicon* **47,** 537-548
50. Menez, A., Bouet, F., Guschlbauer, W., and Fromageot, P. (1980) *Biochemistry* **19,** 4166-4172
51. Endo, T. and Tamiya, N. (1991) Structure-function relationships of postsynaptic neurotoxins from the snake venoms. In Harvey, A. L., editor. *Snake Toxins*, Pergamon Press,
52. Dufton, M. J. and Hider, R. C. (1988) *Pharmacol.Ther.* **36,** 1-40
53. Antil, S., Servent, D., and Menez, A. (1999) *J.Biol.Chem.* **274,** 34851-34858
54. Torres, A. M., Kini, R. M., Selvanayagam, N., and Kuchel, P. W. (2001) *Biochem.J.* **360,** 539-548
55. Ackermann, E. J., Ang, E. T., Kanter, J. R., Tsigelny, I., and Taylor, P. (1998) *J.Biol.Chem.* **273,** 10958-10964
56. Osaka, H., Malany, S., Molles, B. E., Sine, S. M., and Taylor, P. (2000) *J.Biol.Chem.* **275,** 5478-5484
57. Malany, S., Osaka, H., Sine, S. M., and Taylor, P. (2000) *Biochemistry* **39,** 15388-15398
58. Teixeira-Clerc, F., Menez, A., and Kessler, P. (2002) *J.Biol.Chem.* **277,** 25741-25747

59. Bourne, Y., Talley, T. T., Hansen, S. B., Taylor, P., and Marchot, P. (2005) *EMBO J.* **24,** 1512-1522
60. Pillet, L., Tremeau, O., Ducancel, F., Drevet, P., Zinn-Justin, S., Pinkasfeld, S., Boulain, J. C., and Menez, A. (1993) *J.Biol.Chem.* **268,** 909-916
61. Tremeau, O., Lemaire, C., Drevet, P., Pinkasfeld, S., Ducancel, F., Boulain, J. C., and Menez, A. (1995) *J.Biol.Chem.* **270,** 9362-9369
62. Nirthanan, S., Charpantier, E., Gopalakrishnakone, P., Gwee, M. C., Khoo, H. E., Cheah, L. S., Bertrand, D., and Kini, R. M. (2002) *J.Biol.Chem.* **277,** 17811-17820
63. Harvey, A. L. and Rodger, I. W. (1978) *Toxicon* **16,** 219-225
64. Krajewski, J. L., Dickerson, I. M., and Potter, L. T. (2001) *Mol.Pharmacol.* **60,** 725-731
65. Grutter, T. and Changeux, J. P. (2001) *Trends Biochem.Sci.* **26,** 459-463
66. Fruchart-Gaillard, C., Gilquin, B., Antil-Delbeke, S., Le Novere, N., Tamiya, T., Corringer, P. J., Changeux, J. P., Menez, A., and Servent, D. (2002) *Proc.Natl.Acad.Sci.U.S.A* **99,** 3216-3221
67. Barchan, D., Kachalsky, S., Neumann, D., Vogel, Z., Ovadia, M., Kochva, E., and Fuchs, S. (1992) *Proc.Natl.Acad.Sci.U.S.A* **89,** 7717-7721
68. Takacs, Z., Wilhelmsen, K. C., and Sorota, S. (2001) *Mol.Biol.Evol.* **18,** 1800-1809
69. Neumann, D., Barchan, D., Horowitz, M., Kochva, E., and Fuchs, S. (1989) *Proc.Natl.Acad.Sci.U.S.A* **86,** 7255-7259
70. Burden, S. J., Hartzell, H. C., and Yoshikami, D. (1975) *Proc.Natl.Acad.Sci.U.S.A* **72,** 3245-3249

FIGURE LEGENDS

Fig. 1. Isolation, purification and sequencing of denmotoxin. A) LC-MS of *Boiga dendrophila* venom. Crude venom (75 μg) was loaded onto an analytical Jupiter C18 column attached to a Perkin-Elmer Sciex API300 LC/MS/MS. The bound proteins were eluted using a linear gradient (0-90% ACN in 0.05% TFA) at a flow rate of 50 μL/min. Arrow with solid head indicates the peak containing the protein of interest. **B)** Cation exchange chromatography of *Boiga dendrophila* venom. Crude venom (5 mg) was loaded onto a UNO S-6 column equilibrated with 50 mM Tris-HCl buffer, pH. 7.5. Bound proteins were eluted with a linear gradient of buffer B (1 M NaCl in 50 mM Tris-HCl buffer, pH. 7.5). Fraction 2, indicated with an arrow, contains the protein of interest. **C)** RP-HPLC of fraction 2 on C18 Jupiter column using a shallow gradient (30-40% over 80 min) of buffer B (80% ACN in 0.1% TFA). The peak (arrow) contains a single homogenous protein which was named denmotoxin. **D)** ESI/MS of denmotoxin. The spectrum shows a series of multiply charged ions, corresponding to a homogenous protein with a molecular mass of 8507.92 ± 30 Da (inset). **E)** Gel filtration on Superdex 30 column, using 50 mM Tris-HCl, pH 7.4 as eluent, confirmed that denmotoxin is a monomer. Elution volumes of several proteins were plotted against their molecular weight to generate a standard curve. 1 - ovalbumin 45.9 kDa; 2 - ribonuclease 15.6 kDa; 3 - cytochrome C 12 kDa; 4 - apoprotinin 7 kDa; 5 - peloveterin 4 kDa. The molecular weight of denmotoxin was determined by its elution volume (indicated by an arrow). **F)** Determination of amino acid sequence of denmotoxin. The removal of pyroglutamic acid from the NH_2-terminal using pyroGlu aminopeptidase is indicated by an asterisk. NH_2-terminal sequencing of unblocked pyridylethylated protein by Edman degradation is indicated with the solid arrow. Sequences of one Lys-C and two tryptic peptides are indicated by dashed and dashed-dotted arrows, respectively. Sequence deduced from the cDNA sequence is indicated with fine-dotted line.

Fig. 2. Multiple sequence alignment of denmotoxin with **A)** non-conventional toxins and **B)** three-finger toxins. Toxin names, species and Swiss-Prot accession numbers are shown. Cysteines are marked in grey. Disulfide bridges and loop regions are also shown.

Fig. 3. Purification and characterization of synthetic denmotoxin. A) RP-HPLC of reduced crude material on analytical Discovery®BIO Wide Pore C5 (5 μ, 300 Å, 4.6 x 150 mm) eluted with a gradient 40 to 60% of solvent B (A = 0.1% TFA in H_2O; B = 60% ACN and 0.1% TFA in H_2O) in 40 min at a flow of 1mL/min. Arrow indicates peak corresponding to reduced synthetic denmotoxin. **B)** ESI/MS of the purified, synthetic denmotoxin with 10 reduced cysteine residues. The spectrum shows a series of multiply charged ions, corresponding to the correct molecular mass of 8517.38 ± 0.44 Da. **C)** RP-HPLC of refolded synthetic denmotoxin purified on Discovery®BIO Wide Pore C5 (5 μ, 300 Å, 0.1 x 25 cm) column with a gradient of 30 to 50% of solvent B in 40 min (A = 0.1% TFA in H_2O; B = 60% acetonitrile and 0.1% TFA in H_2O). Arrow indicates peak corresponding to properly refolded synthetic denmotoxin. **D)** ESI/MS of refolded, synthetic denmotoxin. The spectrum shows a series of multiply charged ions, corresponding to the correct molecular mass of 8507.70 ± 0.22 Da. **E)** Co-elution of native and synthetic denmotoxin. RP-HPLC on analytical Discovery®BIO Wide Pore C5 (5 μ, 300 Å, 4.6 x 150 mm) column with the gradient 30 - 50% of solvent B in 40 min (A = 0.1% TFA in H_2O; B = 60% acetonitrile and 0.1% TFA in H_2O). The flow rate was 1 mL/min. Profiles of native (top), synthetic (middle) and equimolar mixture of native and synthetic toxin (bottom) are shown; note that all chromatograms show the same elution time.

Fig. 4. Neuromuscular block produced by denmotoxin. A) Segment of tracing showing the irreversible blockage of nerve-evoked twitches produced by denmotoxin (10 μg/mL; 1.176 μM) in the chick biventer cervicis muscle; contractions produced by exogenous acetylcholine (Ach, 300 μM) carbachol (CCh, 8μM) and potassium chloride (KCl, 30 mM), before and after treatment with toxin, are also shown. **B)**

Segment of tracing showing the readily-reversible blockage of nerve-evoked twitches produced by denmotoxin (100 μg/mL; 11.76 μM) in mouse hemidiaphragm. α-bungarotoxin (0.1 μM), however, produces an irreversible block. **C)** Dose-response curves for the neuromuscular block produced by α-bungarotoxin (circles) and denmotoxin (squares) in chick biventer cervicis muscle preparation (filled symbols) and in mouse hemidiaphragm preparation (open symbols) after 30 min of exposure to respective toxins.

Fig. 5. Crystal structure of denmotoxin. A) Stereo view of the overall structure of denmotoxin. Cysteine bonds are shown in yellow. The two phosphate ions and the sodium and potassium ions are shown; **B)** Superimposition of denmotoxin (green) with α-cobratoxin (2CTX - pink) and erabutoxin-b (3EBX - violet). **C)** Surface plot of denmotoxin showing electrostatic potential and the negative tip of the central loop (red).

Fig. 6. Interaction sites between nAChR and postsynaptic neurotoxin. A) Pairwise sequence alignment of the functional loops of α_1, γ and δ subunits of mouse and chicken muscle nAChRs. Loops A, B, and C belong to the α-subunit and constitute the principal component of the plus side of the ligand binding site interface. Loops D, E, and F (γ- and δ-subunit) belong to the complementary component at the minus side of the interface of the ligand binding site. Non-identical residues are shaded in yellow. **B)** α-Cobratoxin (blue) interaction with the complementary face of the AChBP subunit (green) (59). The segment which forms the part of the complementary face between β8 and β9 of AChBP is colored red. Dashed line indicates disordered region in the structure. **C)** Partial sequence of *L. stagnalis* AChBP subunit aligned with equivalent regions of α, γ and δ subunits of chick and mouse muscle AChR. The source of each sequence (Swiss-Prot accession number) is given in brackets. The residues that have 100%, ≥ 75% and ≥ 50% identity are colored in dark blue, marine blue and light blue, respectively. The secondary structural elements (β8 and β9) are shown according to the crystal structure of *L. stagnalis* AChBP (PDB #1UX2). Tip up triangles denote AChBP residues from the complementary faces of the subunit interface that interact with α-cobratoxin (59). Arg193, which may contribute to bird-specificity of denmotoxin, is highlighted in red (For details, see Discussion). Red box indicates AChBP residues (Asp172 – Ser185) colored in red in B.

Table I. Crystallographic data and refinement statistics

Data collection	
Resolution range (Å)	52 - 1.7
Wavelength (Å)	1.006768
Observed reflections >1	50240
Unique reflections	16784
Completeness (%)	93.5
Overall *(I/σI)*	8.5
R_{sym} [a] (%)	10.3
Space group	C2
Cell parameters (Å, °)	98.91 34.04 54.38 90 90 118.36
Refinement	
Resolution range (Å)	47- 1.9
R_{work} [b] (no. of reflections)	20.19 (11487)
R_{free} [c] (no. of reflections)	23.84 (584)
RMSD bond lengths (Å)	0.032
RMSD bond angles(deg)	2.088
Average B-factors (Å^2)	
Main chain	17.05
Side chains	20.83
Ramachandran plot	
Most favored regions (%)	83.1
Additional allowed regions (%)	15.3
Generously allowed regions (%)	1.6
Disallowed regions (%)	0

[a] $R_{sym} = \Sigma|I_i - \langle I \rangle| / \Sigma|I_i|$ where I_i is the intensity of the i^{th} measurement, and $\langle I \rangle$ is the mean intensity for that reflection.

[b] $R_{work} = \Sigma| F_{obs} - F_{calc}| / \Sigma|F_{obs}|$ where F_{calc} and F_{obs} are the calculated and observed structure factor amplitudes, respectively.

[c] R_{free} = as for R_{work}, but for 5% of the total reflections chosen at random and omitted from refinement.

Fig. 1

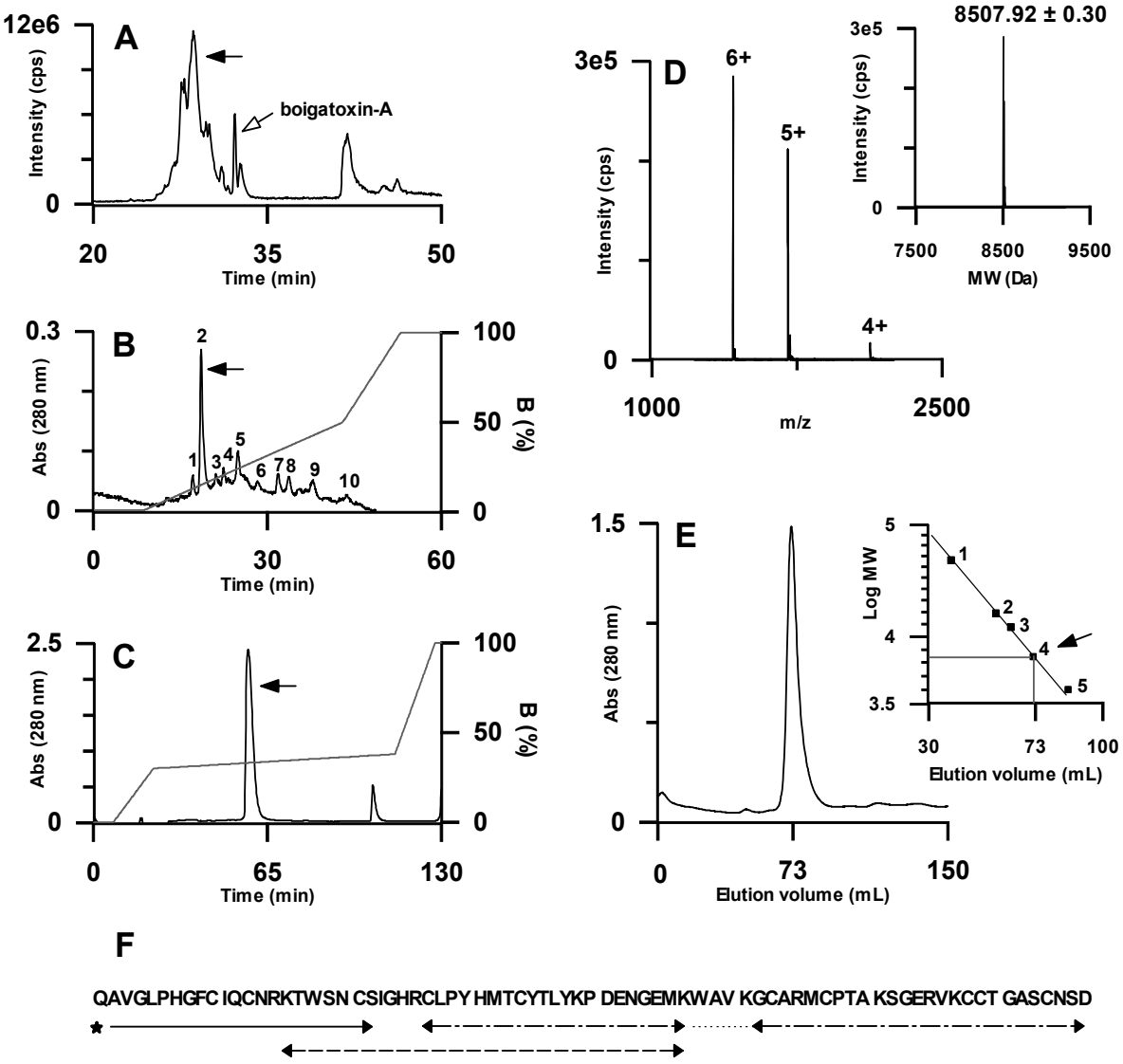

Fig. 2

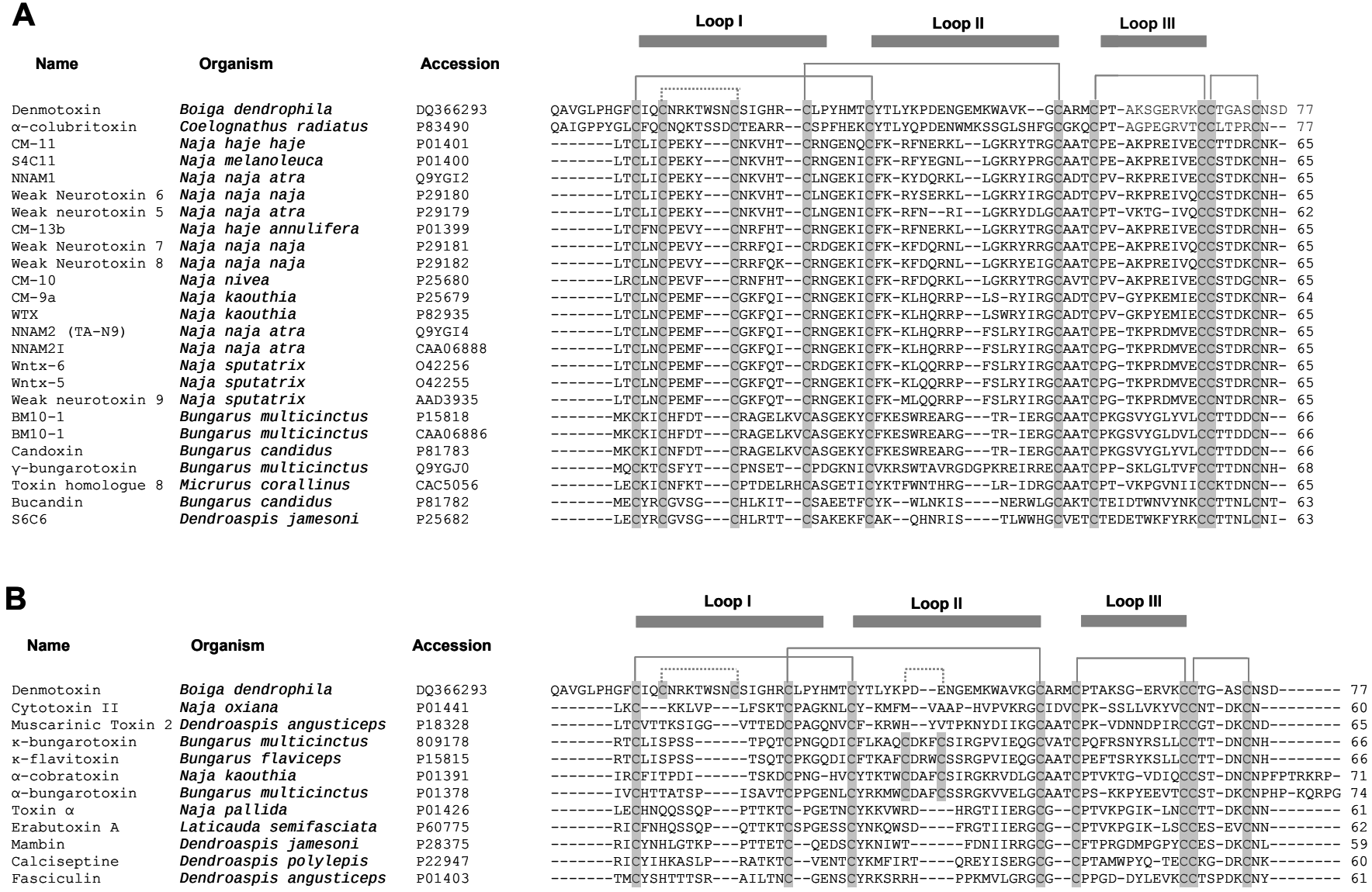

Fig. 3

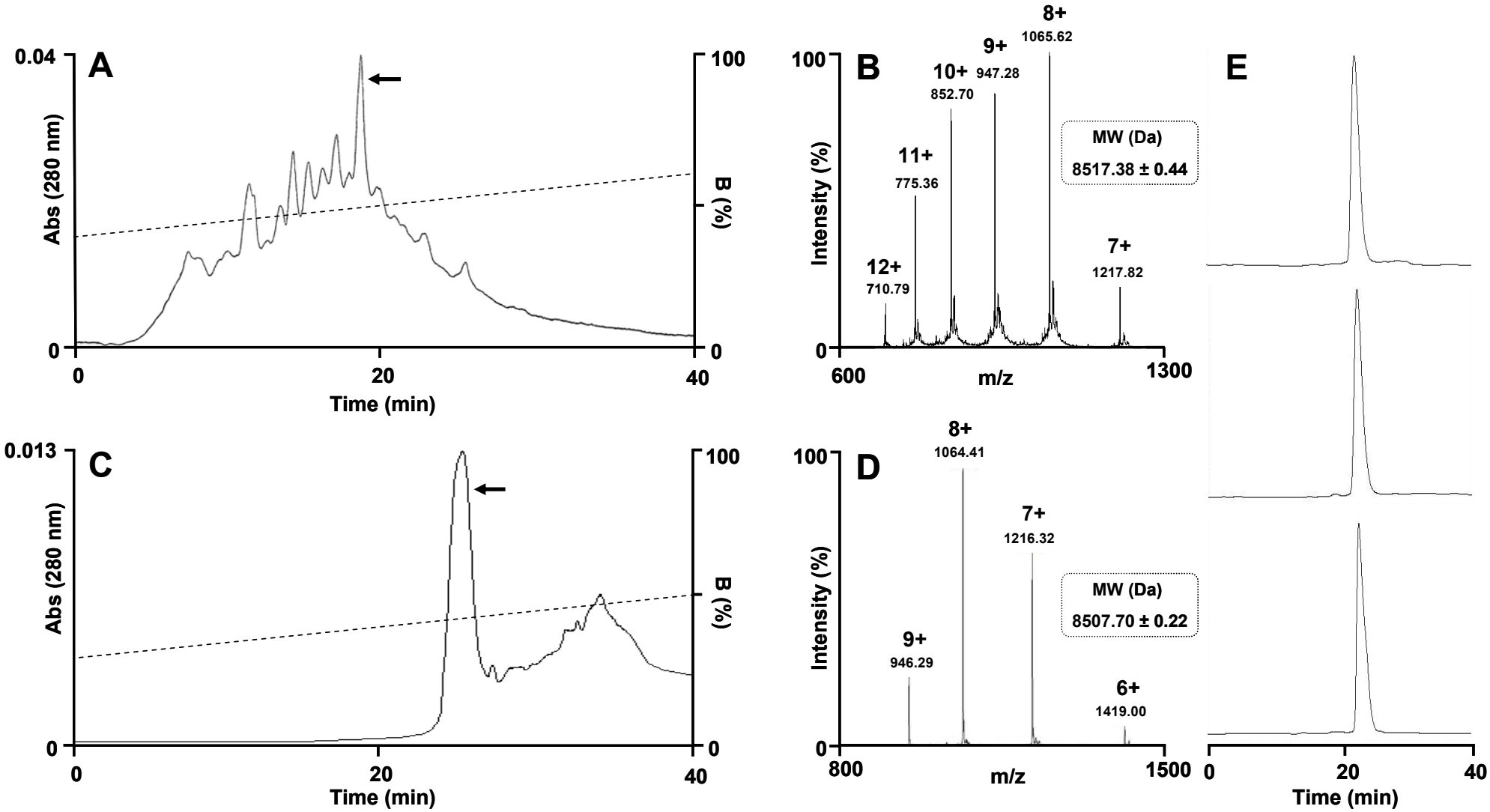

Fig. 4

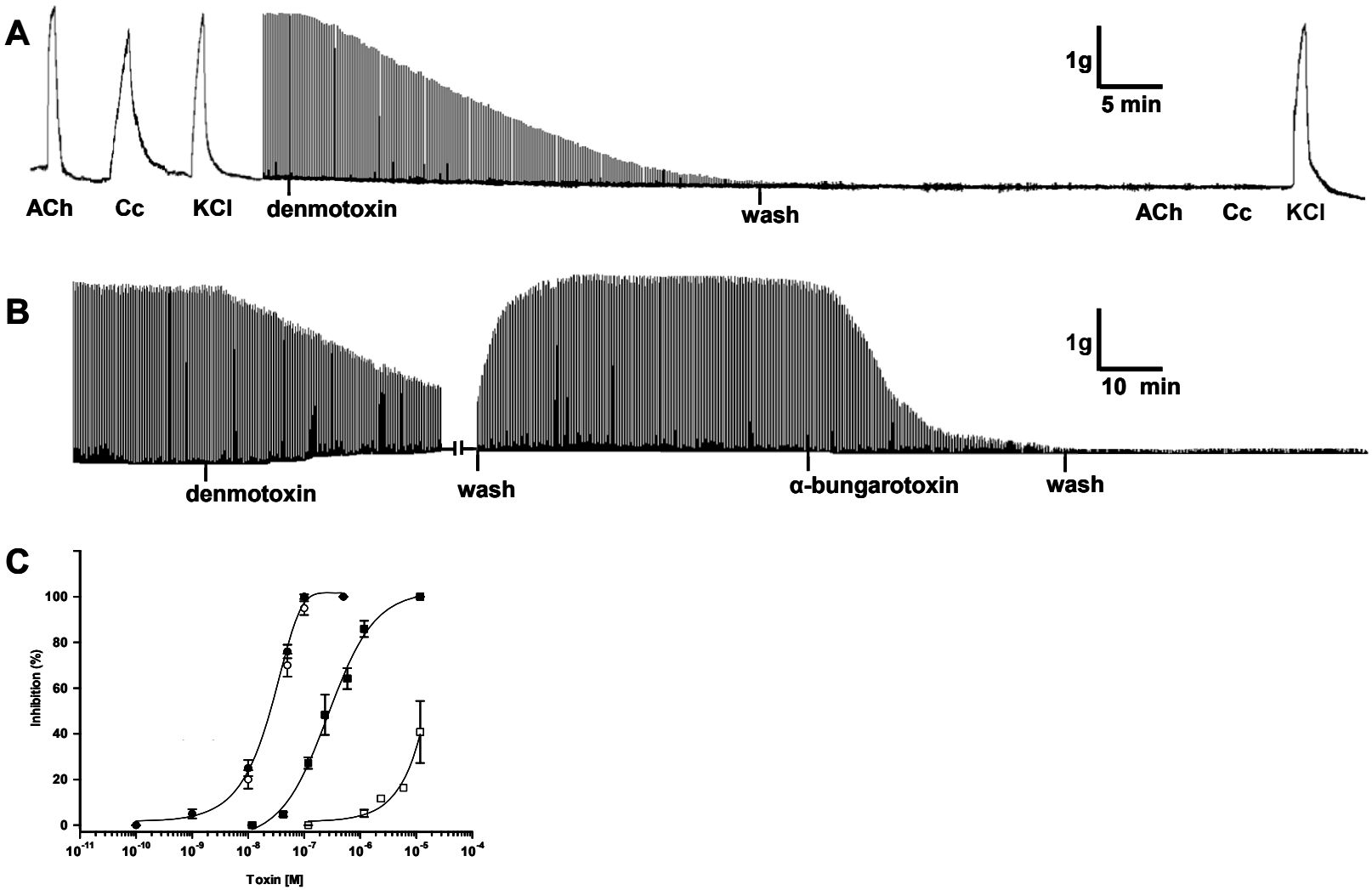

Fig. 5

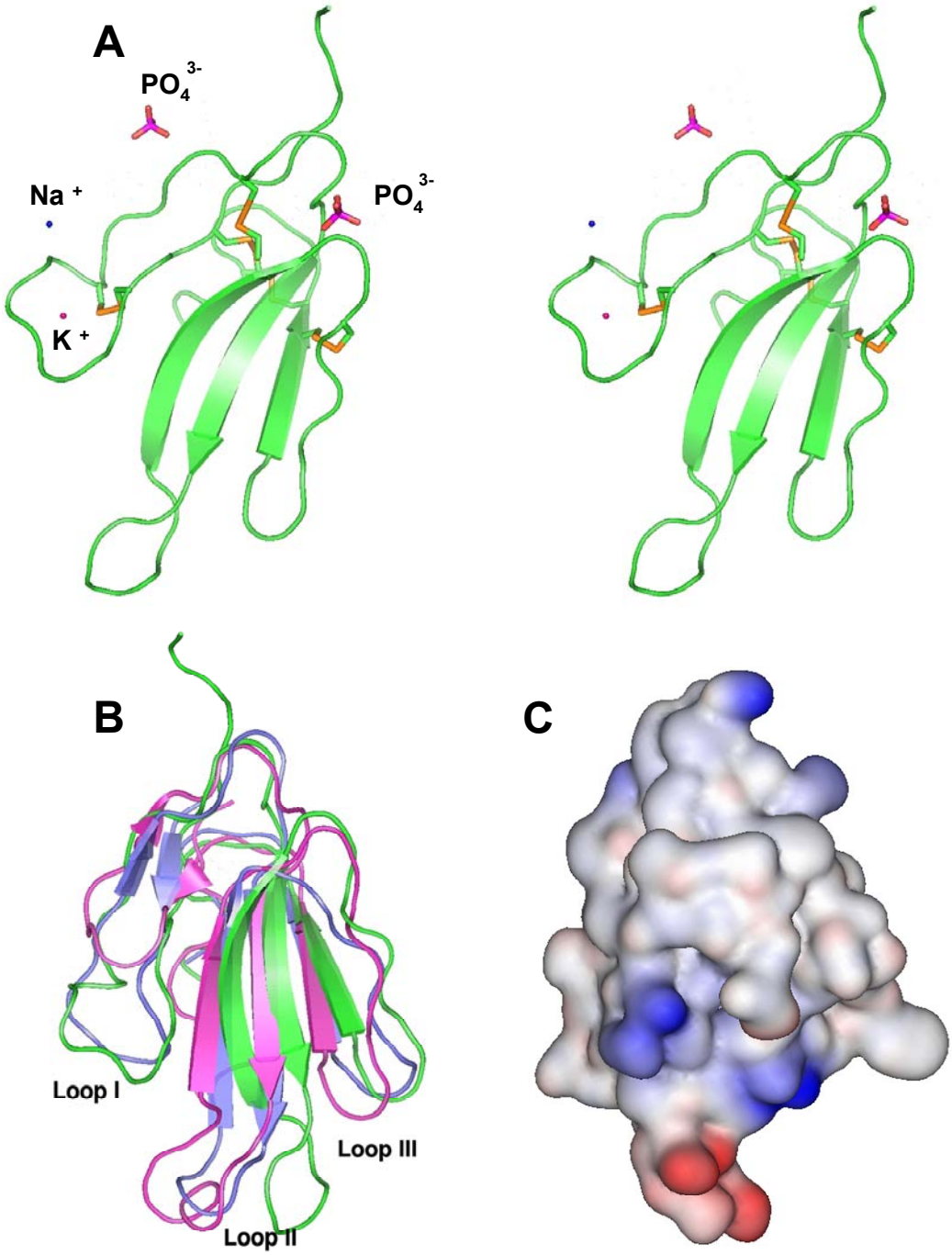

Fig. 6